Available online at www.sciencedirect.com

SciVerse ScienceDirect

journal homepage: www.elsevier.com/locate/he

Investigation of water gas-shift activity of Pt–MO_x–CeO_2/Al_2O_3 (M = K, Ni, Co) using modular artificial neural networks

*M. Erdem Günay, Fatma Akpinar, Z. Ilsen Onsan, Ramazan Yildirim**

Department of Chemical Engineering, Boğaziçi University, Bebek 34342, Istanbul, Turkey

ARTICLE INFO

Article history:
Received 16 August 2011
Received in revised form
22 September 2011
Accepted 28 September 2011
Available online 15 November 2011

Keywords:
Water gas shift reaction
Pt based catalysts
Artificial neural networks
Fuel cells

ABSTRACT

The water gas shift activity of promoted Pt–CeO_2/Al_2O_3 catalysts were investigated in this work. The catalysts were prepared by incipient to wetness impregnation and tested using a microflow reaction system. It was found that K has beneficial effects under product-containing feed compositions while Co and Ni promoters worsen catalyst performance. The reaction temperature and feed H_2O/CO ratio positively affect the catalytic activity, whereas CO_2 and H_2 addition to the feed decreases CO conversion, as expected. The experimental results were also modeled using modular neural networks, at which the catalyst preparation and operational (reaction) variables were used together in the same network because they are interacting but processed differently because they are dissimilar in their form (i.e. categorical versus continuous) and their effects on catalytic activity. It was concluded that the effects of catalyst preparation and operational variables and their relative importance could be comprehended more accurately by using this approach, which may be also employed in other similar systems.

1. Introduction

The world energy demand has continuously increased in recent years due to the increase of world population and living standards. Most of this demand is currently supplied by fossil fuels even though they are quite harmful to the environment, and they are estimated to be depleted in the near future. Thus, new and more sustainable fuel alternatives and energy conversion technologies have been extensively studied in recent years. Fuel cells, which electrochemically convert hydrogen and oxygen to electricity and water, are among the most widely studied subjects in the area of energy systems.

The safe storage of gaseous hydrogen is technically quite difficult today; hence, on-site generation of hydrogen from a conventional fuel using a fuel processor is considered to be the best option in the near future for mobile and small-medium scale stationary applications of fuel cells, especially of Polymer Electrolyte Membrane (PEM) fuel cells [1,2]. However, the hydrogen produced by the reforming process contains CO, CO_2 and H_2O, all of which may affect the performance of the fuel cell. Especially, CO can poison the anode catalyst of the PEM fuel cell even in trace amounts; therefore, it must be eliminated from the hydrogen stream [3,4]. It was suggested that most of the CO can be removed by water-gas shift (WGS) reaction, also producing some additional hydrogen, followed by preferential CO oxidation (PROX) for complete elimination of the remaining about 1% CO [5].

Commercially, WGS is conducted in a two-step process: a high temperature shift (operating at 573–723 K) using Fe–Cr based catalyst, and if necessary, a low temperature shift to

* *Corresponding author*. Tel.: +90 212 359 7248; fax: +90 212 287 2460.
E-mail address: yildirra@boun.edu.tr (R. Yildirim).

0360-3199/$ – see front matter
doi:10.1016/j.ijhydene.2011.09.148

reduce the carbon monoxide content further (operating at 473–523 K) using a Cu–Zn catalyst. However, these catalysts are not suitable for fuel cell applications due to their low activity and stability as well as their special pretreatment and regeneration requirements [5]. Hence, more active and stable WGS catalysts need to be developed for PEM fuel cell applications. Pt, Rh, Pd, Ru and Au supported over CeO_2 and Al_2O_3 [6]; Pt over ceria-zirconia [7]; Cu/Al_2O_3 promoted by Mn [8]; Cu and Ni over CeO_2 [9,10]; Au over ZnO and Fe_2O_3 [11]; Cu–ZnO over Al_2O_3, MgO, SiO_2–Al_2O_3, SiO_2–MgO, β-zeolite, and CeO_2 [12] have been studied for the low temperature WGS studies within the last decade. It is quite clear from the literature that the type of base metal, support, promoter and the preparation conditions may have significant influence on the catalytic activity. The same is true for the operational conditions. Equilibrium-limited and mildly exothermic WGS reaction is thermodynamically favored at temperatures where reaction kinetics is slow; therefore, reaction temperature plays a crucial role in the CO conversions achieved; at low temperatures the reaction is kinetically controlled whereas it is limited by thermodynamic equilibrium at high temperatures [13]. Hence, the effects of catalyst ingredients, catalyst preparation conditions and the operational conditions should be understood and the proper combination of these variables should be selected to develop a catalyst with an acceptable performance. The performances of most WGS catalysts are affected by the reversibility of the reaction and by strong product inhibition.

It is quite difficult to interpret the raw catalytic reaction data due to the complex interactions among the catalyst preparation and operational variables unless a proper tool or method is used. Artificial neural network modeling, which mimics the learning in the biological neurons, can be very useful to overcome this problem. Neural network modeling began to be used extensively in the fields of chemistry and chemical engineering in 1990s. Burns and Whitesides [14] described the use of neural networks with their successful implementations in the area of chemistry in 1993. Similarly, Himmelblau [15] reported numerous works related to the application of neural network modeling in the field of chemical engineering and reviewed some of them in 2000. Hattori and Kito pioneered the application of neural networks in catalysis in mid 1990s [16]. Since then, several successful applications of neural networks were published. For example, Hou et al. applied neural network modeling to find the optimum catalyst ingredients giving the highest acrylonitrile yield for propone ammoxidation catalysts [17] while similar studies were performed by Holena and Baerns for oxidative dehydrogenation of propane to propene [18], by Serra et al. for n-octane isomerization [19] and by Song et al. for catalytic reforming of crude ethanol [20]. In addition, neural networks were used together with some other approaches such as holographic research [21] while some investigators improved the use of neural network itself. For example, Kito and Hattori introduced the partial differentiation method to calculate the relative significances of catalysts variables more accurately [22,23]. We also combined an experimental design method with neural network modeling to analyze the low temperature CO oxidation over promoted Pt/Al_2O_3 data in a more systematic manner [24].

The neural network modeling in catalysis is not limited to the experimental work only. For instance, Omata et al. [25] and Kobayashi et al. [26] used neural networks to virtually screen the effects of new metal additives from their various physicochemical properties for the selective CO oxidation. Similarly, we modeled the data generated by the density functional theory by using artificial neural networks to analyze the behavior of gold clusters on the adsorption of CO and O_2 [27].

The neural networks used in these studies are monolithic in structure, meaning that the input variables are processed in the same manner in a fully connected way. However, catalyst preparation and operational variables are quite different in their nature and their differences should be taken into account in modeling. Modular neural networks, which divide the problem into subtasks [28,29] and process them separately, such as using different activation functions in each module, can be more accurate for this purpose, as demonstrated in one of our previous communications [30]. The catalyst preparation and the operational variables can be collected into two different groups in a modular network allowing them to be used together but processed differently so that their effects on the activity of the catalyst can be understood and predicted better.

In this work, we have experimentally studied the WGS activity of 1 wt% Pt-1.25 wt% Ce/Al_2O_3 catalysts in the absence and presence of a 1.25 wt% second promoter (K, Ni, Co), and analyzed our results by means of modular neural networks to demonstrate that this technique can be used to predict the results of unstudied conditions as well as to understand the effects of catalyst preparation and operational conditions. We chose this catalyst system for two reasons: First, it seems from the literature that Pt/CeO_2 is a promising combination for the WGS reaction. Second, the addition of a second metal promoter has worked well in preferential CO oxidation (PROX) as previously reported [24,30–32], and we wanted to test the possibility of using a similar catalyst for WGS because this will significantly facilitate the use of WGS and PROX reactor combinations.

2. Materials and methods

2.1. Catalyst preparation

The catalysts were prepared using the classical incipient to wetness co-impregnation technique [31]. $Pt(NH_3)_4(NO_3)_2$ (Aldrich), $Ce(NO_3)_3 6H_2O$ (Merck), $Co(NO_3)_2\ 6H_2O$ (Merck), K_2CO_3 (Merck) and $Ni(NO_3)_2.6H_2O$ (Merck) were used as precursors. 250–355 μm commercial γ-alumina was calcined at 450 °C for 5 h prior to impregnation, which was put in a vacuum flask and kept under vacuum both before and during the addition of precursor solution. The required volume of precursor solution was slowly pumped to the vacuum flask. The slurry was mixed by an ultrasonic mixer for 90 min during the impregnation in order to maintain uniform distribution of the precursor solution; it was then dried in an electric oven at 105 °C for 16 h and calcined under the conditions given in Table 1.

Table 1 – Calcination procedures of catalysts.

Catalyst	Calcination temperature (C)	Calcination time (hr)
Pt–Ce/Al_2O_3	400	2
Pt–Ce–K/Al_2O_3	450	1
Pt–Ce–Ni/Al_2O_3	450	2
Pt–Ce–Co/Al_2O_3	400	2

2.2. *Activity measurements*

The activities of the catalysts were measured using a micro-reactor flow system. Research grade CO, H_2, CO_2 and He were used, and their flowrates were controlled using Brooks 5850E mass flow controllers. The water was pumped into the preheated (150 °C) reactant gas mixture using a Jasko PU-2080Plus HPLC pump and evaporated in a glass wool bed before reaching the catalyst. The feed mixture was allowed to flow through the 4 mm ID stainless steel fixed-bed reactor. Reactor temperature was controlled by a Shimaden FP-21 programmable controller in a 40 cm × 2.4 cm ID tube furnace. The feed flow rate was kept constant at 100 cm^3/min. The 0.25 g catalyst samples used in the experiments were reduced *in situ* at 400 °C in a hydrogen environment for 3 h before each activity measurement. All experiments were performed at atmospheric pressure, and the data were taken continuously and analyzed using a Hiden HPR 20 QIC mass spectrometer.

2.3. *Computational details*

Experimental water gas shift reaction results comprising 138 data points were modeled by artificial neural networks created in the MATLAB 7.10 (R2010a) environment. The range and type of the input variables in two groups (catalyst preparation and operational variables) and the output variable (CO conversion) are given in Table 2.

Backpropagation algorithm with delta rule of error correction was applied as the learning algorithm to adapt the weights of the neural network [33,34], while the method of steepest descent was used as the optimization method for training. Each neural network topology was trained three times in order to compensate for the random initialization of the neural network weights, and the best performances were recorded. Root mean square error (RMSE) and coefficient of determination (R^2) values were used to evaluate and compare the statistical fitness of the networks [24,35]. The RMSE of training was determined by using the entire database as the training data for the neural network. On the other hand, the RMSE of testing was calculated by k-fold cross validation method [18,27,30] with a "k" value of four. The entire database was randomly divided into four subsets. Data belonging to the three subsets were used to train the neural network to predict the output of the remaining one set (unseen data). The procedure was repeated four times until all the subsets were tested. The differences between the neural network predictions and the experimental results covering all the four subsets were used to determine the RMSE of testing, which is a measure of how well the neural network can predict the outcome of a new set of conditions (generalization accuracy) [36–38]. RMSE of testing was used as the criteria to determine the optimal neural network topology best representing the catalytic data.

Table 2 – The range and type of input and output variables used.

	Input variable	Range
preparation variables	promoter type	Ce, K, Ni
operational variables	reaction temperature (°C)	250–300
	CO_2 content (%)	0–10
	H_2 content (%)	0–40
	H_2O/CO ratio	2–3
	TOS (min)	30–180
output variable	CO conversion (%)	0–80.6

The time on stream (TOS) does not change the main character of the catalyst or catalyst reaction conditions; it is just an indicator of the time of measurement (and partially the indicator of stability). Thus, while applying k-fold cross validation method, the data over a particular catalyst at all TOS values were excluded from the training set; otherwise, the neural network would have used the CO conversion value at one time on stream to estimate the conversion at another time, which would have caused a testing error smaller than the actual error [24,30].

The optimal neural network topology with the minimum testing error was found initially by using the logistic sigmoid function as the activation (transfer) function in the hidden layers of the network [39]. Then, various activation functions were tested for the catalyst preparation and the operational variables separately (as one of the advantages of the modular approach) to improve the generalization accuracy of the network [30].

The relative significances of the continuous variables were found by partial differentiation of the fully trained neural network. This method was reported to give reliable results for analyzing the variable significances, and the full procedure of the method can also be found in the previously published studies [22,23]. On the other hand, the method of "change of root mean square error" [24,30,40] was used to test the significance of the categorical input variables (promoter type) since the method of partial differentiation cannot be applied to categorical data. The procedure in this approach starts with the removal of the first input variable from the input list, and the neural network is trained with the remaining variables (i.e. it is forced to predict the output without using the excluded input variable). This procedure is repeated for all the input variables, and the training RMSE values obtained this way are compared with the RMSE obtained from the model that is trained with all the inputs. The differences are used as the indicator of the relative significances of each variable (sum is normalized to 100), as the larger difference means that corresponding input variable is more significant (because its exclusion causes larger deviation from the original model) [24,30,40]. The relative group significances of preparation and operational variables were also computed using the change of mean square error method.

3. Results and discussion

In this section, the experimental results for all catalyst are summarized first without any detailed discussion about the catalyst preparation and reaction conditions, since they will be extensively discussed in the following sections. Then, the optimal network topology that represents the experimental data will be presented. Finally, the effects of catalyst preparation and operational variables on CO conversion will be discussed in detail followed by the analysis of relative significances of these variables.

3.1. Experimental results

The experimental results obtained at 300 °C and 60 min of TOS over all catalysts and feed conditions are summarized in Fig. 1. The 1 wt% Pt–1.25 wt% Ce/Al_2O_3 catalyst gave about 80% conversion with the feed composition of 5% CO and 10% H_2O (equilibrium conversion is about 98%). All the second metal additives (1.25 wt%) tested had negative impacts on activity under these conditions. However, Ni and K addition improved CO conversion in the presence of 10% CO_2 in the feed, and the improvement in case of K was quite significant (almost 10%). It should also be noted that the performance of K-containing catalyst did not change with the addition of CO_2 even though CO conversion dropped in all the other cases. The effect of 40% H_2 in feed was more dramatic, causing a significant decrease in the CO conversion over all catalysts. The K-containing catalyst was still the best with 28% CO conversion in the presence of hydrogen. The simultaneous addition of 10% CO_2 and 40% H_2 decreased the CO conversion further over all catalysts, as expected; however, Pt–Ce–K/Al_2O_3 lost its advantage against Pt–Ce/Al_2O_3, leading to almost the same CO conversion level of about 20%. The results under various temperatures, TOS values and feed conditions are discussed in Section 3.3 together with model predictions.

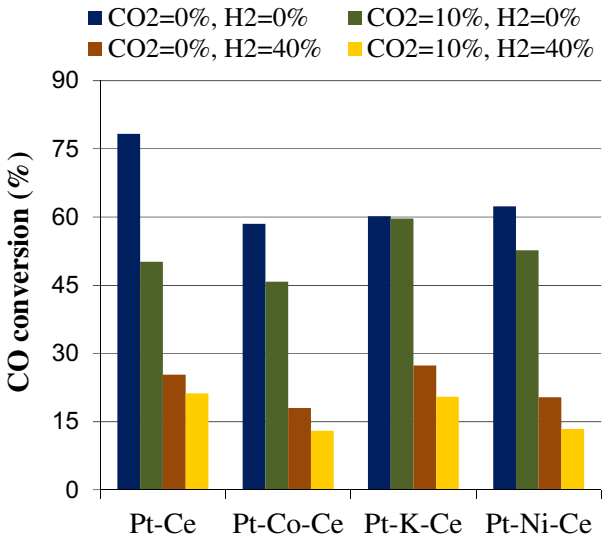

Fig. 1 – Effect of catalyst composition on CO conversion at 300 °C and 60 min of TOS. Feed: 5% CO, 10% H_2O with balance He.

3.2. Determination of the optimal artificial neural network model

In order to find the optimal neural network topology that may best represent the experimental data, nine modular neural networks with different topologies were constructed. The statistical approximation accuracies of training and testing of these networks are shown in Fig. 2. The notation of "(a-b)-c" is used to label the neural networks, where "a" represents the number of the first hidden layer neurons connected to the preparation variables (promoter type), similarly "b" represents the first hidden layer neurons connected to the operational variables, c is the number of neurons in the second hidden layer. There are eight input variables and one output variable, which is the CO conversion.

The training errors (gray bars in Fig. 2) were calculated by using the entire data set for training. On the other hand, the testing errors (black bars) were calculated by applying 4-fold cross validation as explained in Section 2.2. According to Fig. 2, the training error decreases as the neural network model gets larger due to the use of more weights to represent the data [38], while the testing error first decreases and then tends to increase because of the increase in the degree of overlearning [24,30,36,37]. Among the networks analyzed, the network with the topology of (2-3)-3 (Fig. 3) was chosen as the topology (testing RMSE = 5.22) with the highest generalization ability, which is the indicator of network's ability to predict the data not seen before.

This network was improved further by using different activation functions in the modules of the first hidden layer. All the nine combinations of logistic sigmoid function (lsf), hyberbolic tangent function (tanh) and identity function (ide) [39] were tested for the modules of catalyst preparation and operational variables while the logistic sigmoid function was kept in the second hidden layer (Fig. 4).

It was found that the network with the topology (2-3)-3 was improved significantly with the use of identity function for the preparation variables and hyperbolic tangent function for the operational variables. The training and the testing RMSE of this network were calculated as 1.99 and 3.36 respectively. The experimental versus predicted CO conversion plots for both training and testing data are given in Fig. 5. The data are distributed around the y = x lines with very high R^2 values for both plots indicating that the neural network model

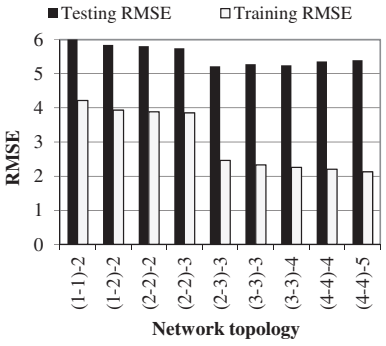

Fig. 2 – Testing and training errors for various neural network topologies.

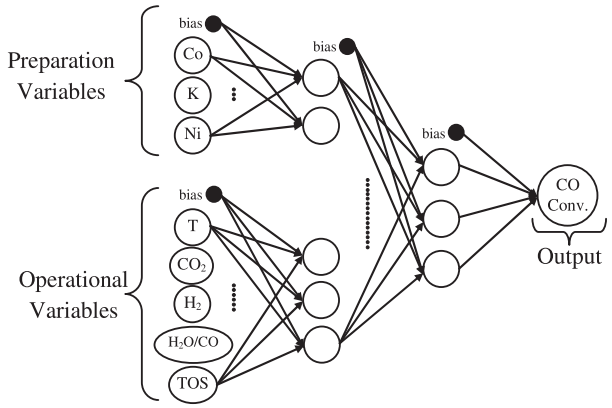

Fig. 3 – Topology of the optimum neural network model.

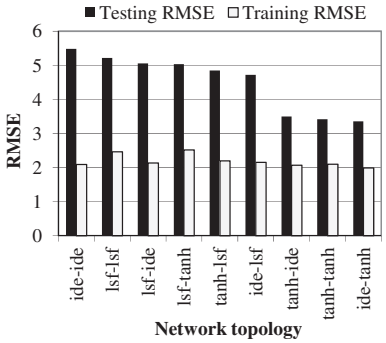

Fig. 4 – Testing and training errors of the (2-3)-3 neural network topology with different activation functions for the preparation and the operational variables.

constructed is quite successful in predicting the data. Especially, the fitness of the testing plot (Fig.5(b)) is quite remarkable considering that each predicted CO conversion in this plot was made by the network which did not see that point during training. The optimal neural network topology proposed here was used for the remaining part of the analysis.

3.3. *Prediction of the effects of catalyst preparation and operational variables*

Fig. 6 compares the predicted and the experimental CO conversions versus TOS for all the catalysts in the absence and presence of H_2 or/and CO_2. The predictions are generally very close to the experimental values, which is a further indicator for the success of the model. Although neural networks have superior ability in predicting the nonlinear effects of variables, the model predictions in this case are almost linear because the experimental CO conversions are not significantly influenced by the change of TOS. The prediction of slight nonlinearity could be improved by employing a larger network topology; however the use of the smallest network capturing the general trends was preferred to keep the generalization ability higher as discussed in Section 3.2.

It is quite apparent from Fig. 6 that the presence of H_2 decreases CO conversion significantly for all the catalysts due to the reverse WGS reaction, which consumes CO_2 and H_2 producing CO and H_2O. For the same reason, the presence of CO_2 also decreases the WGS activity though its effect seems to be smaller in the present case, actually due to the small feed concentration of this component compared to hydrogen. When both CO_2 and H_2 are present in the reaction stream (realistic stream composition exiting a reformer), the catalytic activity reduces even more. It is also apparent from Fig. 6 that the activities of all catalysts slightly decrease with increasing TOS which may be an evidence for possible deactivation.

In the absence of CO_2 and H_2, the catalyst with the best performance is the Pt–Ce catalyst (without any second promoter), which was proposed as a very good catalyst for WGS reaction due to the high oxygen storage capacity of ceria and its ability of stabilizing the support and the noble metal [9]. On the other hand, the addition of any of the promoters Co, K, Ni had a detrimental effect in the absence of CO_2 and H_2. However, a good water gas shift reaction catalyst has to work in the presence of significant levels of CO_2 and especially H_2 [41,42]. Hence, all the catalysts were also tested in the presence of these components, and it was

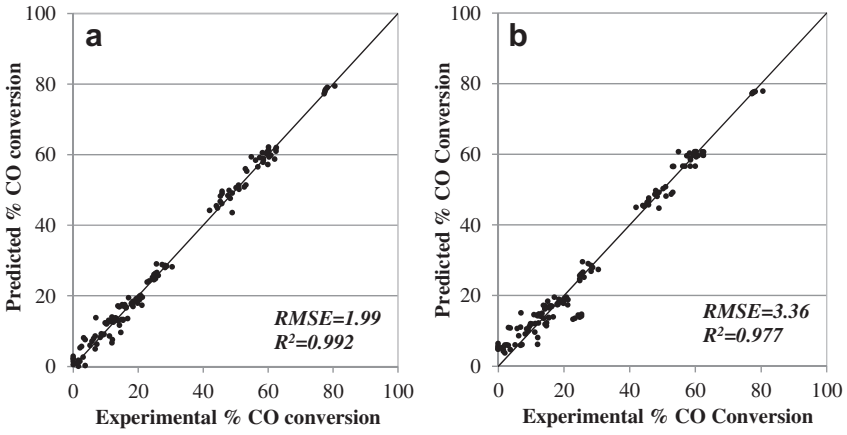

Fig. 5 – Experimental versus predicted CO conversion values: (a) training, (b) testing; for the modular network of (2-3)-3 with the activation functions of "ide-tanh" in the first hidden layer.

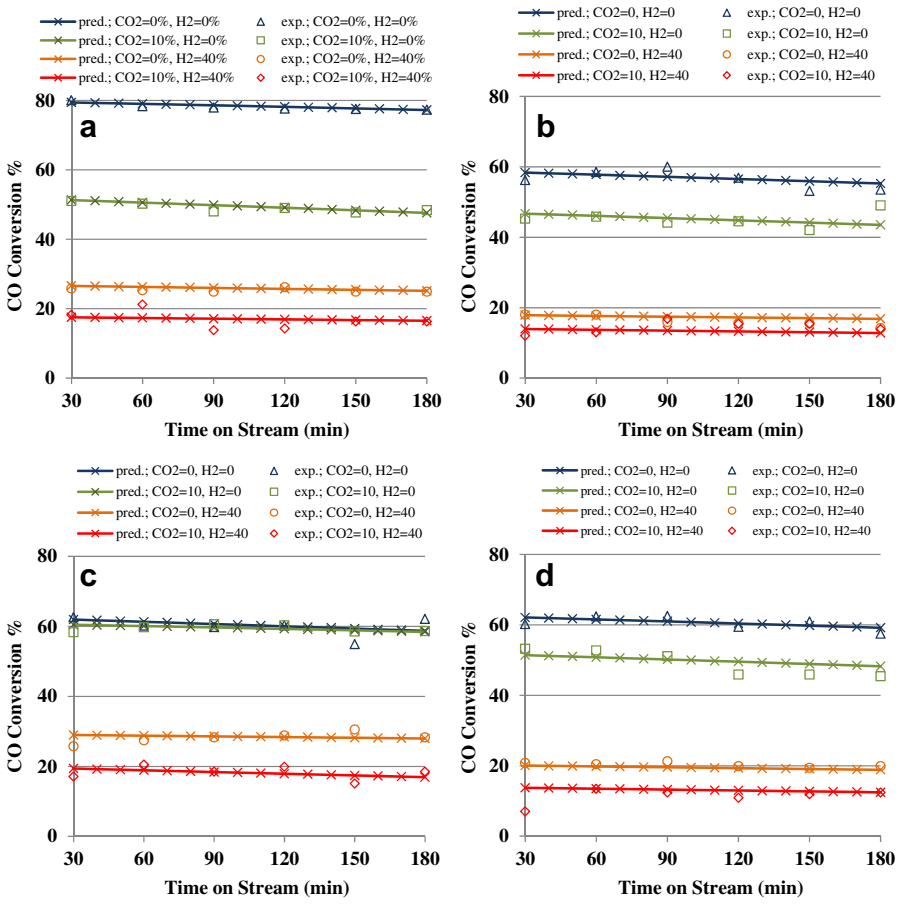

Fig. 6 – CO conversion versus TOS at 300 °C in various reaction streams for: (a) Pt–Ce, (b) Pt–Co–Ce, (c) Pt–K–Ce, (d) Pt–Ni–Ce, Pt.

found that the Pt–Ce–K catalyst was less affected from CO_2 and/or H_2 in contrast to the Pt–Ce–Co and Pt–Ce–Ni catalysts. When only CO_2 was present in the reaction stream, Pt–Ce–K had significantly higher activity even compared to Pt–Ce. The performance of the Pt–Ce–K catalyst was almost the same (slightly better) as the Pt–Ce catalyst when both CO_2 and H_2 were present. The Pt–Ce–K catalyst can be analyzed further in future studies, since it may be superior to the Pt–Ce catalyst under some other operational conditions.

The predicted and the experimental performances of Pt–Ce, Pt–Co–Ce and Pt–K–Ce catalysts at different temperatures under realistic conditions are given in Fig. 7, which shows that decreasing the reaction temperature has

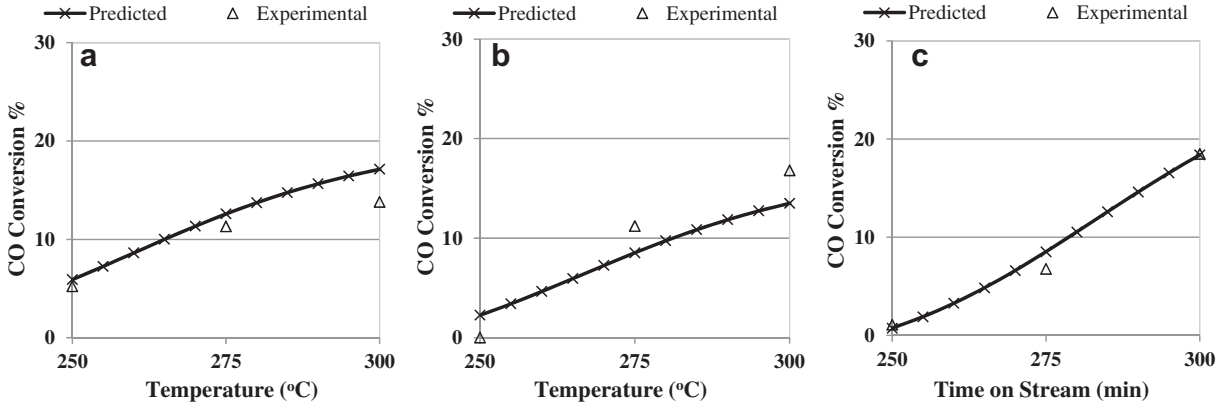

Fig. 7 – CO conversion versus reaction temperature in the presence of 10% CO_2 and 40% H_2 at 90 min of TOS for: (a)Pt–Ce, (b) Pt–Co–Ce, (c)Pt–K–Ce.

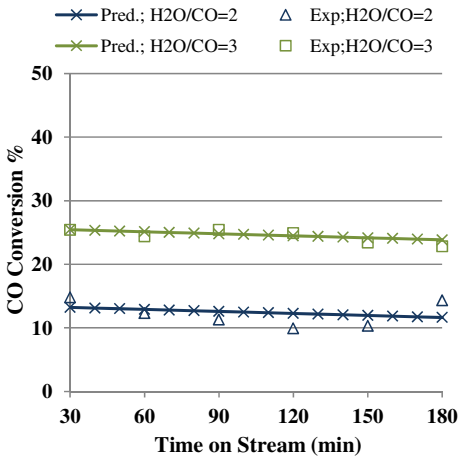

Fig. 8 – Effect of H_2O/CO ratio on catalyst activity in the presence of 10% CO_2 and 40% H_2 at 275 °C for Pt–Ce.

a negative effect on CO conversion. This is expected because, although WGS is an exothermic reaction (equilibrium constant increases with decreasing temperature), it also becomes kinetically controlled at lower temperatures which prevents the approach to thermodynamic limits [13,43]. The effects of temperature on all the catalysts are quite successfully predicted by the neural network model.

Finally, the effect of H_2O/CO ratio in the feed on CO conversion over the Pt–Ce catalyst at 275 °C is shown in Fig. 8 as a sample case. The increase in the H_2O/CO ratio positively affects the catalytic activity as also reported by various previous studies [44,45]. The promotion of WGS is due to the shifting of reaction equilibrium to the product side by the presence of excess water and was also successfully predicted by the network model.

Normally, the neural network can be optimized to find the input variables maximizing CO conversion. However, it was not necessary in the present case because it is evident that higher temperatures and H_2O/CO ratios would increase CO conversion. On the other hand, the lower values of these variables are more desirable for the heat and water management in fuel cell systems. Hence, the optimization of the neural network was omitted for this case.

3.4. *Relative significance of catalyst preparation and operational variables*

Table 3 shows the relative significances of the catalyst preparation and the operational variables. It is to be noted that these significances should be treated within the range of conditions studied; otherwise, they may produce misleading conclusions. For example, the relative significance of the temperature indicates its relative influence over CO conversion between the lowest to highest values selected in the study; if the reaction temperature were set to very low values (like room temperature), no CO conversion would be obtained and the temperature would have a much higher relative significance. This is also true for all the other variables.

Under the conditions studied, the group significance of the operational variables was found to be 81.7% while the second promoter addition was 18.3%. This is quite reasonable since the Pt–Ce catalyst has a certain level of performance, and the second promoter has a minor impact. On the other hand, the chances of temperature and feed composition to influence CO conversion are significant. Among the operational variables, H_2 percentage was the most significant because it increased reverse WGS reaction decreasing the CO conversion severely. The presence of CO_2 had the same effect with lesser degrees due to its smaller percentage in the feed.

The H_2O/CO ratio was the second most significant operational variable; increasing this ratio was expected to increase the water gas shift catalytic activity considerably [44,45]. The influence of TOS was not found significant because it had only some minor impact on CO conversion due a very slight activity loss. This is also apparent in Fig. 6, which shows that CO conversions do not decrease significantly even after 3 h of operation for all the catalysts. The low relative significance value (9.4%) for the operation temperature can be attributed to the fact that experimental analysis was conducted in a narrow temperature range compatible with actual operating conditions used in fuel processors.

Table 3 – Relative significances of the catalyst preparation and the operational variables.

	Variables	RMSE without the variable	RMSE difference[a]	% Relative significance (change of RMSE method)	% Relative significance (partial differentiation)	Group significance (change of RMSE method)
preparation variables	Co	4.11	2.13	40.0		18.3
	K	3.79	1.81	34.0		
	Ni	3.37	1.38	26.0		
operational variables	React T				9.4	81.7
	CO_2				10.7	
	H_2				43.7	
	H_2O/CO				33.3	
	TOS				2.9	

a Difference between "RMSE without the variable" – "RMSE of the original model (1.99)."

4. Conclusions

The effects of second promoter (K, Co and Ni) on the water gas shift activity of Pt–CeO_2/Al_2O_3 catalyst were investigated experimentally, and the results were analyzed computationally using modular neural networks. It was found that K has some beneficial effects under product-containing feed compositions, while Co and Ni promoters worsen catalyst performance. The reaction temperature and feed H_2O/CO ratio positively affect the catalytic activity, whereas CO_2 and H_2 addition to the feed decrease CO conversion, as expected.

The modular neural network model successfully predicted the effects of promoter type and operational variables, and revealed that, under the conditions studied, H_2 concentration and H_2O/CO ratio in the feed are the most significant variables determining the catalytic performance. It was also found that the effects of catalyst preparation and operational variables and their relative importance could be comprehended more accurately by using modular neural networks, at which these two groups of variables were used together in the same network but processed differently. These results suggested that modular neural networks may be used to analyze similar systems to capture the effects and significances of reaction variables, and they may improve and expedite experimental studies.

Acknowledgments

Financial supports provided by TÜBİTAK through Project 105M034 and Boğaziçi University through BAP-06M104 are gratefully acknowledged.

REFERENCES

[1] Luengnaruemitchaia A, Osuwana S, Gulari E. Selective catalytic oxidation of CO in the presence of H_2 over gold catalyst. Int J Hydrogen Energy 2004;29:429–35.
[2] Trimm DL, Onsan ZI. Onboard fuel conversion for hydrogen-fuel-cell-driven vehicles. Catal Rev 2001;43:31–84.
[3] Choudhary TV, Goodman DW. CO-free fuel processing for fuel cell applications. Catal Today 2002;77:65–78.
[4] Park ED, Lee D, Lee HC. Recent progress in selective CO removal in a H_2-rich stream. Catal Today 2009;139:280–90.
[5] Onsan ZI. Catalytic processes for clean hydrogen production from hydrocarbons. Turk J Chem 2007;31:531–50.
[6] Panagiotopoulou P, Kondarides DI. Effect of the nature of the support on the catalytic performance of noble metal catalysts for the water–gas shift reaction. Catal Today 2006; 112:49–52.
[7] Lim S, Bae J, Kim K. Study of activity and effectiveness factor of noble metal catalysts for water–gas shift reaction. Int J Hydrogen Energy 2009;34:870–6.
[8] Yeragi DC, Pradhan NC, Dalai AK. Low-temperature water-gas shift reaction over Mn-promoted Cu/Al_2O_3 catalysts. Catal Lett 2006;112:139–48.
[9] Li Y, Fu Q, Flytzani-Stephanopoulos M. Low-temperature water-gas shift reaction over Cu- and Ni- loaded cerium oxide catalysts. Appl Catal B 2000;27:179–91.
[10] Kim SH, Chung JH, Kim YT, Han J, Yoon SP, Nam SW, et al. SiO_2/Ni and CeO_2/Ni catalysts for single-stage water gas shift reaction. Int J Hydrogen Energy 2010;35:3136–40.
[11] Tabakova T, Idakiev V, Andreeva D, Mitov I. Influence of the microscopic properties of the support on the catalytic activity of Au/ZnO, Au/ZrO_2, Au/Fe_2O_3, Au/Fe_2O_3–ZnO, Au/Fe_2O_3–ZrO^2 catalysts for the WGS reaction. Appl Catal A 2000;202:91–7.
[12] Yahiro H, Murawaki K, Saiki K, Yamamoto T, Yamaura H. Study on the supported Cu-based catalysts for the low-temperature water–gas shift reaction. Catal Today 2007;126: 436–40.
[13] Mhadeshwar AB, Vlachos DG. Is the water–gas shift reaction on Pt simple? Computer-aided microkinetic model reduction, lumped rate expression, and rate-determining step. Catal Today 2005;105:162–72.
[14] Burns JA, Whitesides GM. Feed-forward neural networks in chemistry: mathematical systems for classification and pattern recognition. Chem Rev 1993;93:2583–99.
[15] Himmelblau DM. Applications of artificial neural networks in chemical engineering. Korean J Chem Eng 2000;17:373–92.
[16] Hattori T, Kito S. Neural network as a tool for catalyst development. Catal Today 1995;23:347–55.
[17] Hou Z-Y, Dai Q, Wu X-Q, Chen G- T. Artificial neural network aided design of catalyst for propane ammoxidation. Appl Catal A 1997;161:183–90.
[18] Holena M, Baerns M. Feedforward neural networks in catalysis a tool for the approximation of the dependency of yield on catalyst composition, and for knowledge extraction. Catal Today 2003;81:485–94.
[19] Serra JM, Corma A, Chica A, Argente E, Botti V. Can artificial neural networks help the experimentation in catalysis? Catal Today 2003;81:393–403.
[20] Song S, Akande AJ, Idem RO, Mahinpey N. Inter-relationship between preparation methods, nickel loading, characteristics and performance in the reforming of crude ethanol over Ni/Al_2O_3 catalysts: a neural network approach. Eng Appl Artif Intel 2007;20:261–71.
[21] Tompos A, Margitfalvi JL, Tfirst E, Végvári L. Information mining using artificial neural networks and "holographic research strategy". Appl Catal A 2003;254:161–8.
[22] Kito S, Hattori T. Analysis of catalytic performance by partial differentiation of neural network pattern. Chem Eng Sci 2007;62:5575–8.
[23] Hattori T, Kito S. Partial differentiation of neural network for the analysis of factors controlling catalytic activity. Appl Catal A 2007;327:157–63.
[24] Günay ME, Yildirim R. Neural network aided design of Pt–Co–Ce/Al_2O_3 catalyst for selective CO oxidation in hydrogen-rich streams. Chem Eng J 2008;140:324–31.
[25] Omata K, Kobayashi Y, Yamada M. Artificial neural network-aided design of Co/$SrCO_3$ catalyst for preferential oxidation of CO in excess hydrogen. Catal Today 2006;117:311–5.
[26] Kobayashi Y, Omata K, Yamada M. Screening of additives to a Co/$SrCO_3$ catalyst by artificial neural network for preferential oxidation of CO in excess H_2. Ind Eng Chem Res 2010;49:1541–9.
[27] Davran-Candan T, Günay ME, Yıldırım R. Structure and activity relationship for CO and O_2 adsorption over gold nanoparticles using density functional theory and artificial neural networks. J Chem Phys 2010;132:174113. 1-9.
[28] Melin P, Mancilla A, Lopez M, Mendoza O. A hybrid modular neural network architecture with fuzzy Sugeno integration for time series forecasting. Appl Soft Comput 2007;7: 1217–26.
[29] Kang S, Isik C. Partially connected feedforward neural networks structured by input types. IEEE Trans Neural Netw 2005;16:175–84.

[30] Günay ME, Yildirim R. Analysis of selective CO oxidation over promoted Pt/Al_2O_3 catalysts using modular neural networks: combining preparation and operational variables. Appl Catal A 2010;377:174–80.
[31] Ince T, Uysal G, Akin AN, Yildirim R. Selective low-temperature CO oxidation over $Pt–Co–Ce/Al_2O_3$ in hydrogen-rich streams. Appl Catal A 2005;292:171–6.
[32] Uguz KE, Yildirim R. Comparative study of selective CO oxidation over $Pt–Co–M/Al_2O_3$catalysts (M = Ce, Mg, Mn, Zr, Fe) in hydrogen-rich streams: effects of a second promoter. Turk J Chem 2009;33:545–53.
[33] Callan R. The essence of neural networks. Hertfordshire: Prentice Hall; 1999.
[34] Larose DT. Discovering knowledge in data. New Jersey: Wiley; 2005.
[35] Günay ME, Nikerel IE, Oner ET, Kirdar B, Yildirim R. Simultaneous modeling of enzyme production and biomass growth in recombinant Escherichia coli using artificial neural networks. Biochem Eng J 2008;42:329–35.
[36] Cundari TR, Deng J, Zhao Y. Design of a propane ammoxidation catalyst using artificial neural networks and genetic algorithms. Ind Eng Chem Res 2001;40:5475–80.
[37] Molga E. Neural network approach to support modelling of chemical reactors: problems, resolutions, criteria of application. J Chem Eng Process 2003;42:675–95.
[38] Khajeh-Hosseini-Dalasm N, Ahadian S, Fushinobu K, Okazaki K, Kawazoe Y. Prediction and analysis of the cathode catalyst layer performance of proton exchange membrane fuel cells using artificial neural network and statistical methods. J Power Sources 2011;196:3750–6.
[39] Mandic DP, Chambers JA. Recurrent neural networks for prediction. London: Wiley; 2001.
[40] Sung AH. Ranking importance of input parameters of neural networks. Expert Syst Appl 1998;15:405–11.
[41] Zou H, Dong Z, Lin W. Selective CO oxidation in hydrogen-rich gas over CuO/CeO_2 catalysts. Appl Surf Sci 2006;253: 2893–8.
[42] Ayastuy JL, Gurbani A, Gonzalez-Marcos MP, Gutiérrez-Ortiz MA. Effect of copper loading on copper-ceria catalysts performance in CO selective oxidation for fuel cell applications. Int J Hydrogen Energy 2010;35:1232–44.
[43] Thinon O, Diehl F, Avenier P, Schuurman Y. Screening of bifunctional water-gas shift catalysts. Catal Today 2008;137: 29–35.
[44] Caglayan BS, Aksoylu AE. Water-gas shift reaction over bimetallic $Pt–Ni/Al_2O_3$ catalysts. Turk J Chem 2009;33: 249–56.
[45] Figueiredo RT, Ramos ALD, de Andrade HMC, Fierro JLG. Effect of low steam/carbon ratio on water gas shift reaction. Catal Today 2005;107–108:671–5.